

## Modes of Periodic Domain Wall Motion in Ultrathin Ferromagnetic Layers

W. Kleemann,\* J. Rhensius, and O. Petracic†

Angewandte Physik, Universität Duisburg-Essen, D-47048 Duisburg, Germany

J. Ferré and J. P. Jamet

Laboratoire de Physique des Solides, Université Paris-Sud, UMR CNRS 8502, 91405 Orsay, France

H. Bernas

CSNSM, Université Paris-Sud, UPR CNRS 6412, 91405 Orsay, France

(Received 21 March 2007; published 29 August 2007)

Magnetization reversal in a periodic magnetic field is studied on an ultrathin, ultrasoft ferromagnetic Pt/Co(0.5 nm)/Pt trilayer exhibiting weak random domain wall (DW) pinning. The DW motion is imaged by polar magneto-optic Kerr effect microscopy and monitored by superconducting quantum interference device susceptometry. In close agreement with model predictions, the complex linear ac susceptibility corroborates the dynamic DW modes segmental relaxation, creep, slide, and switching.

DOI: 10.1103/PhysRevLett.99.097203

PACS numbers: 75.60.Ch, 62.20.Hg, 75.60.Jk, 75.70.Ak

Quenched randomness in ferroic systems (e.g., ferromagnets or ferroelectrics) containing domain walls (DWs) has fundamental consequences on their response to an external conjugate field. Depending on the strength of a driving dc field,  $H$ , the DWs exhibit different states of motion below and above the “depinning” field,  $H_p$ . As shown schematically in Fig. 1(a), it separates the regions of thermally activated *creep* ( $H < H_p$ ) and friction-limited viscous *slide* ( $H > H_p$ ) [1–3]. Although the stationary states of creep, *depinning*, and slide under static external fields are meanwhile understood [4], rigorous theoretical results on dynamic states in alternating fields are scarce. An oscillating driving field,  $H = H_0 \exp(i\omega t)$ , initiates additional states of motion at finite angular frequencies,  $\omega > 0$ . On one hand, at constant temperature,  $T > 0$ , and fixed field amplitude,  $H_0$ , segmental domain wall relaxation (“*relaxation*” for short) without net wall motion occurs at high frequencies [5]. On the other hand, at low frequencies the wall dynamics finally turns into periodic *switching* between differently poled states provided that  $H_0$  overcomes coercivity [6]. It should be noticed that very similar phenomena are encountered in high- $T_c$  superconductors, where vortices may undergo pinning and creep as reflected among others by ac susceptibility spectra [7].

In this Letter, direct experimental evidence of all the dynamic modes, viz., relaxation, creep, slide, and switching, is given for the first time on a suitable ferromagnetic (FM) system. To this end we have studied the complex linear ac susceptibility,  $\chi = \chi' - i\chi''$ , of a magnetically Ising-like soft ultrathin FM layer with perpendicular anisotropy, whose magnetization reversal is dominated by DW motion. In such films, weakly pinned DW propagation and magnetization reversal have previously been investigated under stationary conditions,  $H = \text{const}$  [2], or via dynamical magnetization loops,  $M(H[t])$  [8,9]. Our method of probing the dynamic behavior makes use of

the spectral signatures of  $\chi = \chi(\omega)$ , where  $\omega = 2\pi f$  with the frequency  $f$ . The above four dynamic modes are mirrored by typical shapes of the so-called Cole-Cole diagrams,  $\chi''$  vs  $\chi'$  [10], as shown schematically in Fig. 1(b). This was first verified in “*superferromagnetic*” multilayers of  $\text{Co}_{80}\text{Fe}_{20}$  nanoparticles embedded in amorphous alumina,  $\text{Al}_2\text{O}_3$  [11–13]. The Cole-Cole fingerprint identification of relaxation and creep has also proven successful in periodically poled uniaxial ferroelectric  $\text{KTiOPO}_4$  [14].

The Cole-Cole signatures of the different dynamic regimes are understood as follows [15]. Relaxation refers to the polydispersive response of DW segments smaller than the Larkin pinning length,  $L_p$ , which defines the shortest length of the DW controlled by the density of pinning centers via the fluctuations of their random pinning forces [16]. These segments oscillate between local free energy minima without net DW displacement or velocity [6,11]. In the Cole-Cole plot this corresponds to a flattened semi-circle [marked “R” in Fig. 1(b)] at low ac field and high

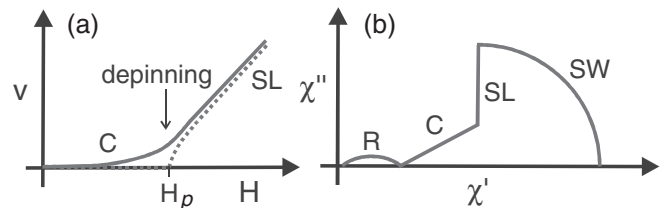


FIG. 1. (a) Schematic plot of the DW velocity,  $v$  vs dc field  $H$ , which does not report on the high-field behavior, exhibiting depinning at  $H = H_p$  and slide (marked as SL) at  $T = 0$  (broken line) and—additionally—creep (C) at  $T > 0$  (solid line). (b) Schematic Cole-Cole plot of the susceptibility components,  $\chi''$  vs  $\chi'$ , due to a randomly pinned DW in ac driving fields, exhibiting relaxation (R), creep (C), slide (SL), and switching (SW).

frequencies. Here, low (or high) field refers to  $H$  smaller (or larger) than the frequency dependent coercive field,  $H_c(f)$ .

Creep denotes the nonadiabatic, i.e., the nonergodic regime, where inner (“minor”) hysteresis loops are cycled at low field and velocity hysteresis is encountered [12,17]. One finds an inverse power-law for the complex susceptibility,  $\chi(\omega) = \chi_\infty[1 + (i\omega\tau)^{-\beta}]$ , hence, a linear dependence,  $\chi'' = (\chi' - \chi_\infty) \tan(\pi\beta/2)$ , marked “C” in Fig. 1(b). Here  $\beta$  is a polydispersivity exponent,  $0 < \beta < 1$ ,  $\tau$  a characteristic relaxation time and  $\chi_\infty$  the limiting value for  $\omega \rightarrow \infty$ .

The transition between relaxation and creep is readily understood when considering the general relation for the susceptibility of a weakly pinned DW segment of length  $L$  with a curvature of radius  $R$ , magnetic moment  $m_0$ , and interface stiffness  $\Gamma$  [5],

$$\chi(\omega) = \frac{m_0^2 L^2}{R\Gamma} \frac{1}{1 + i\omega\tau(L)}. \quad (1)$$

$L$  either scales with the frequency of the ac field or remains constant beyond the depinning frequency  $\omega_p$ , respectively, as [18]

$$L = \begin{cases} L_p (\frac{\omega_p}{\omega})^{1/z} & \omega < \omega_p \\ L_p & \omega > \omega_p \end{cases} \quad (2)$$

with the dynamical exponent  $z$ .

Since weak pinning takes place on all scales above  $L_p$ , the susceptibility finds contributions at all frequencies  $\omega < \omega_p$ , weighted by a density of states,  $g(L) \propto L^{-2\zeta}$ , where  $\zeta \approx 2/3$  is the roughening exponent [4]. The principal contributions of the DW segments satisfy the condition  $\omega\tau = 1$ , hence,  $\tau \propto L^z$ . Thus, Eq. (2) yields the heterogeneously broad susceptibility function by weighting with  $g(L)$ , substituting  $L$  by Eq. (3) and  $\omega\tau = 1$  [15]:

$$\chi \propto g(L)\chi(L) \propto L^{2-2\zeta} \frac{1}{1 + i\omega\tau(L)} \propto \begin{cases} (\frac{1-i}{2})\omega^{-(2-2\zeta/z)} & \omega < \omega_p \\ \frac{1}{1+i\omega\tau(L_p)} & \omega > \omega_p \end{cases}. \quad (3)$$

As a result, a Debye law is predicted in the relaxation regime,  $\omega > \omega_p$ . Owing to the finite width of the distribution function of the pinning length scale,  $g(L_p)$ , polydispersive broadening may occur. It usually gives rise to flattening of the Debye semicircle as observed, e.g., in  $\text{KTiOPO}_4$  [14]. Empirically it can often be described by a Cole-Cole dispersion law,  $\chi(\omega) = \chi_\infty[1 + (i\omega\tau)^{1-\alpha}]^{-1}$  with  $\alpha < 1$  [10].

On the other hand, in the creep regime,  $\omega < \omega_p$ , we find a power law as described above, where  $\chi_\infty = m_0^2 L^2 / R\Gamma$  denotes the bulk background susceptibility. Obviously the creep exponent satisfies the relationship  $\beta = (2 - 2\zeta)/z$ . Hence, when inserting the dynamical exponent  $z \approx 2(1 - \varepsilon/9)$  [18], where  $\varepsilon = 4 - D$  with the wall dimension  $D$ ,

we expect  $\beta = (2 - 2\zeta)/1.3 \approx 0.5$  for a 1D wall in a 2D ultrathin magnetic film.

The inner loops cycled in the slide regime at lower frequencies and high fields are dominated by adiabatic (= ergodic) “viscous” DW motion [12]. The complex susceptibility is, again, described by the creep equation, however, with  $\beta = 1$ . Hence, disorder becomes irrelevant and the dynamic susceptibility is purely imaginary and contributes a vertical segment (“SL”) to the Cole-Cole plot. In this case, the system can successfully be modeled assuming one DW with a quasistationary dependence of the mean velocity on the applied field,  $v \propto H$  [12]. This contrasts with the creep regime, where modeling has to consider the full equation of motion of a one-dimensional elastic interface in a two-dimensional random medium [6,12,17].

Finally, switching refers to the range, where complete magnetization reversal occurs during cycles in high field. In the Cole-Cole plot it is reasonably well approximated by a low frequency quarter circle (“SW”) [11,12]. Indeed, in the picture of a periodically swept DW only half a Debye semicircle with apex at  $f = 1/2\pi\tau$  is expected to appear. For angular frequencies  $\omega > 1/\tau$  one half of a field cycle, i.e., the time the DW needs to move from one side to the other, is shorter than the intrinsic relaxation time of switching. Under this condition the system does not switch, but rather remains in the slide regime.

The sample studied is a high quality ultrathin magnetic trilayer, Pt(3.5 nm)/Co (0.5 nm)/Pt (4.5 nm), with perpendicular anisotropy, sputtered in high vacuum onto a  $\text{Al}_2\text{O}_3(0001)$  substrate at room temperature [19]. Its static coercive field at  $T = 300$  K was lowered to  $\mu_0 H_c \approx 0.4$  mT by uniform  $\text{He}^+$ -ion beam irradiation at an energy of 30 keV and a fluence of  $F = 1.5 \times 10^{16}$   $\text{He}^+/\text{cm}^2$  [20]. Thus successful switching experiments prove possible within our ac susceptometer based on a superconducting quantum interference device (SQUID, Quantum Design MPMS-5S). Its copper coil for ac fields provides a maximum amplitude  $\mu_0 H_0 = 0.42$  mT at frequencies  $10^{-2} < f < 10^3$  Hz. ac susceptibility is measured in zero field after reducing the residual field at the sample location to below 2  $\mu\text{T}$  by quenching the superconducting solenoid and compensating for remanent fields.

The dominance of domain wall motion under weak ac fields at low- $f$  has been inspected with  $P$ -MOKE microscopy at room temperature. Figure 2 (upper panels 1 to 5) shows five temporally equidistant ( $\Delta t = 2.5$  s) domain configurations (size  $200 \times 150 \mu\text{m}^2$ ) recorded during 1.4 periods of a quasistationary hysteresis cycle at  $f = 0.1$  Hz. They are driven into an oscillating mode by a sinusoidal field with an amplitude  $\mu_0 H_0 = 0.45$  mT (Fig. 2, lower panel). Moderate DW amplitudes,  $\Delta x \approx 50 \mu\text{m}$ , at typical creep velocities,  $\approx 10^{-5} \text{ms}^{-1}$ , are observed. Because of weak pinning, the observed roughness of the DWs gradually increases from period to period [21]. Partially reversible avalanches corroborate heterogeneous DW nucleation

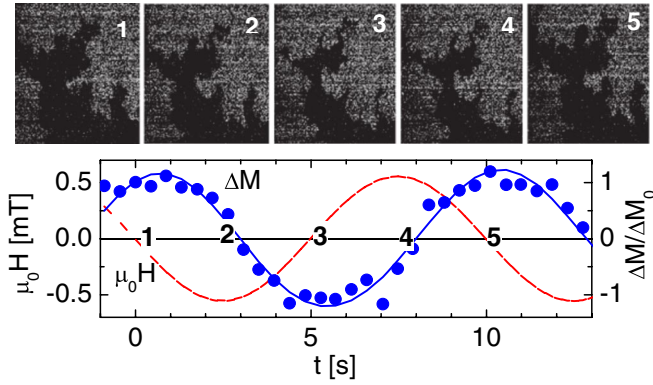


FIG. 2 (color online). Upper panel: *P*-MOKE micrographs (size  $200 \times 150 \mu\text{m}^2$ ) of a Pt/Co(0.5 nm)/Pt trilayer taken at time distances  $\Delta t = 2.5$  s during 1.4 periods of an ac excitation at  $f = 0.1$  Hz with  $\mu_0 H_0 = 0.45$  mT and  $f = 0.1$  Hz. Lower panel: Oscillating magnetic field  $\mu_0 H$  and magnetization  $\Delta M$  vs  $t$  with time labels 1–5 corresponding to the images in the upper panel.

at fluctuations of the quenched random bonds during the periodic excitation.

The oscillating magnetization,  $\Delta M/\Delta M_0$ , is integrated every 0.5 s within an area of  $310 \times 388 \mu\text{m}^2$  over all “up” (“black”) and “down” (“white”) magnetized domains, where  $2\Delta M_0$  denotes the difference between the extremes, 1 and 3 (Fig. 2, lower panel). As expected from the extremely nonlinear  $v$  vs  $H$  dependence [Fig. 1(a)] the largest variations of the magnetization occur at the summits of  $\mu_0 H$ , while  $M$  flattens around  $H = 0$ . Closer inspection reveals an average phase shift between both curves below  $90^\circ$ , which complies with the phase angle  $\beta\pi/2$  expected for creep, where  $\beta < 1$ . Susceptibility data discussed below indicate  $\beta \approx 0.8$ .

In order to identify the above introduced different dynamic DW modes, the complex linear ac susceptibility  $\chi(\omega) = \chi' - i\chi''$  was recorded at constant temperatures,  $275 \leq T \leq 350$  K. Although this very first component of the full Fourier expansion is only a poor approximation in the case of hysteretical  $M$  vs  $H$  loops with highly nonlinear behavior at larger field amplitudes, it was shown previously [12] that  $\chi(\omega)$  reveals meaningful and characteristic signatures in all dynamic regimes. Figure 3 shows spectra of the real,  $\chi'$ , and imaginary part,  $\chi''$ , of the ac susceptibility vs frequency,  $f$ , at  $T = 325$  [panels (a),(b)] and 350 K (d),(e), for three ac amplitudes,  $\mu_0 H_0 = 0.42$ , 0.2 and 0.1 mT. The noisy spectra taken at lower temperatures at the detection limit of the susceptometer are not shown.

It should be noticed that the conditions “high” and “low” field in comparison with the quasistatic coercive field, i.e.,  $H \geq H_c$ , can be controlled either isothermally by varying  $\mu_0 H_0$  at  $T = \text{const}$  (see above) or isomagnetically by varying  $T$  at  $\mu_0 H_0 = \text{const}$ . “Hysteresis hardening” is found on decreasing the temperature, since the static coercive field increases with decreasing temperature,  $\mu_0 H_c = 0.03, 0.11, 0.36$  mT for  $T = 350, 325,$  and

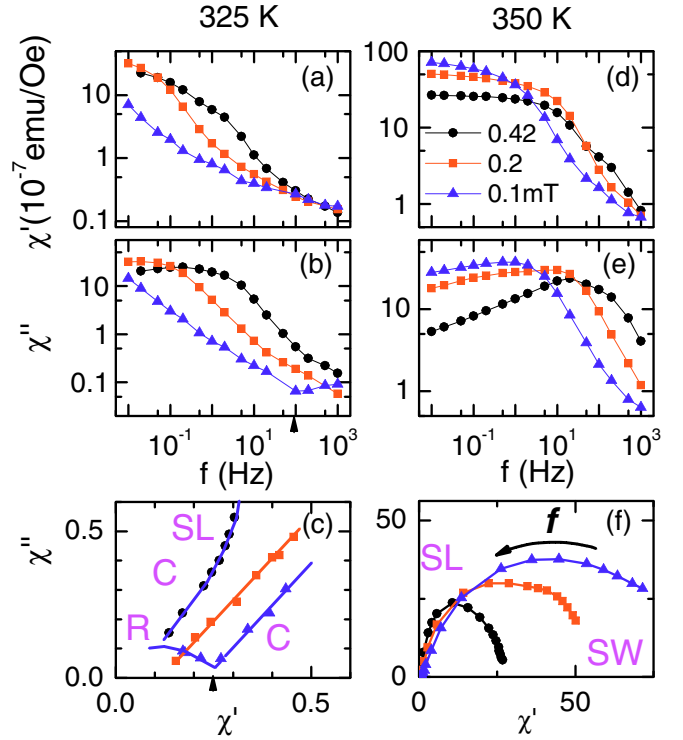


FIG. 3 (color online). Spectra of the real,  $\chi'$ , and imaginary part,  $\chi''$ , of the ac susceptibility vs. frequency,  $f$ , at  $T = 325$  (a),(b) and 350 K (d),(e) for ac amplitudes,  $\mu_0 H_0 = 0.42$  (black circles), 0.2 (red squares) and 0.1 mT (blue triangles), and the corresponding Cole-Cole plots,  $\chi''$  vs  $\chi'$  (c),(f). Bold solid lines mark the power-law creep spectra in (c) and the switching quarter circles in (f). Arrows in (b),(c) mark the relaxation-to-creep crossover. Thin solid lines are guides to the eye.

300 K, respectively. While at  $T = 350$  K, i.e., close to the Curie temperature,  $T_c \approx 370$  K, all of our field amplitudes suffice to operate switching, at  $T = 325$  K they primarily activate creep.

In Fig. 3(d) and 3(e), at 350 K, one clearly observes dispersion steps in the real and—complementarily to this—peaks in the imaginary parts. These features match perfectly with results obtained from simulations of a driven DW in a random medium [12] and signify monodisperse switching, which shifts to lower frequencies with decreasing amplitudes and decreasing temperatures. They mark the crossover from switching to DW slide and creep occurring at higher  $f$  [Fig. 1(b)]. As a rule, this crossover occurs at lower  $f$ —i.e., at lower sweep rates—as lower  $H_0$  or  $T$  are chosen. Indeed, at  $T = 325$  K, the switching spectra shift to very low frequencies, while power-law-like creep spectra,  $\chi'(f)$  and  $\chi''(f)$ , Eq. (2), dominate [best seen in panels (a) and (b)].

The mode signatures are best recognized in the Cole-Cole plots (c) and (f). The curve for  $T = 350$  K and  $\mu_0 H_0 = 0.42$  mT [Fig. 3(f)] matches perfectly with the curve shown in Fig. 6 of Ref. [12]. For low frequencies one observes the expected Cole-Cole quarter circle, which corresponds to the switching regime as indicated in the



plot. For increasing frequencies one enters a steep slide and then (unresolved) the flatter creep regime. For smaller amplitudes, the slide regime is broader and rounded, probably due to the multidomain situation, which evolves quite generally after many field cycles (see Fig. 2).

Isothermal control of the dynamic DW modes via  $\mu_0 H_0$  is clearly seen at  $T = 325$  K [Fig. 3(c)], although creep is dominating as indicated by linear relationships  $\chi'' \propto \chi' - \chi_\infty$  (denoted as “C”) for all field amplitudes. From the slopes  $\tan(\pi\beta/2) = 1.4 \pm 0.2$ ,  $1.5 \pm 0.2$  and  $1.6 \pm 0.2$  [cf. Eq. (3)], we deduce [18]  $\beta = (2 - 2\zeta)/z = 0.6 \pm 0.1$ ,  $0.7 \pm 0.1$ , and  $0.8 \pm 0.1$  for  $\mu_0 H_0 = 0.1$ ,  $0.2$ , and  $0.42$  mT, respectively. Inserting  $z = 1.3$  for a 1D wall in a 2D ultrathin magnetic film [18] we obtain a roughening exponent  $\zeta = 0.6 \pm 0.1$ , in reasonable agreement with the theoretical value,  $\zeta = 2/3$ , as already measured in a similar nonirradiated film [2]. Distinct from creep we notice in Fig. 3(c) that the increasing slope for  $\mu_0 H_0 = 0.42$  mT at low  $f$  hints at the onset of slide (“SL”), while the observed bending of the  $\mu_0 H_0 = 0.1$  mT data into a negative slope at high  $f$  indicates the segmental relaxation regime (“R”). To the best of our knowledge, this regime, being well known from ferroelectric domain systems [14], has now for the first time been observed in an ultrathin FM film. The observed sharp crossover from creep to relaxation reflects the fact that the spectrum of dynamically active domain wall segments condenses to the pinning length,  $L_p$ , when exceeding the threshold frequency, i.e.,  $f_p \approx 100$  Hz for  $\mu_0 H_0 = 0.1$  mT at  $T = 325$  K [arrows in Figs. 3(b) and 3(c)].

In conclusion, we have studied periodic magnetization reversal due to DW dynamics of an ultrathin ferromagnetically soft Ising-like Pt/Co(0.5 nm)/Pt film by imaging the DWs with dynamic  $P$ -MOKE microscopy and by measuring the complex ac SQUID susceptibility. The sample is a nearly ideal model system for a 2D random bond ferromagnet showing all four regimes of DW dynamics—relaxation, creep, slide, and switching. They are identified by their specific signatures in Cole-Cole plots of the linear susceptibility,  $\chi''$  vs  $\chi'$ , which completely characterizes the different modes even in regimes of large nonlinear and hysteretic response. It will be interesting to extend these investigations into the high-field region beyond the Walker breakdown [22], where precessional dynamics replaces the viscous slide motion [23].

Thanks are due to X. Chen, Th. Kleinefeld, and S. A. Prosandeev for discussions and technical help, to P. Metaxas for critical re-reading of the manuscript, and to V. Mathet for preparing the high quality Pt/Co/Pt film.

\*Author to whom correspondence should be addressed.  
wolfgang.kleemann@uni-due.de

<sup>†</sup>Present address: Lehrstuhl für Experimentalphysik, Ruhr-Universität Bochum, 44780 Bochum, Germany.

- [1] M. V. Feigel'man, V. B. Geshkenbein, A. I. Larkin, and V. M. Vinokur, Phys. Rev. Lett. **63**, 2303 (1989).
- [2] S. Lemerle, J. Ferré, C. Chappert, V. Mathet, T. Giamarchi, and P. Le Doussal, Phys. Rev. Lett. **80**, 849 (1998).
- [3] T. Tybell, P. Paruch, T. Giamarchi, and J.-M. Triscone, Phys. Rev. Lett. **89**, 097601 (2002).
- [4] P. Chauve, T. Giamarchi, and P. Le Doussal, Phys. Rev. B **62**, 6241 (2000).
- [5] T. Nattermann, Y. Shapir, and I. Vilfan, Phys. Rev. B **42**, 8577 (1990).
- [6] T. Nattermann, V. Pokrovsky, and V. M. Vinokur, Phys. Rev. Lett. **87**, 197005 (2001).
- [7] G. Blatter, M. V. Feigel'man, V. B. Geshkenbein, A. I. Larkin, and V. M. Vinokur, Rev. Mod. Phys. **66**, 1125 (1994).
- [8] B. Raquet, R. Mamy, and J. C. Ousset, Phys. Rev. B **54**, 4128 (1996).
- [9] T. A. Moore and J. A. C. Bland, J. Phys. Condens. Matter **16**, R1369 (2004).
- [10] K. S. Cole and R. H. Cole, J. Chem. Phys. **9**, 341 (1941); A. K. Jonscher, *Dielectric Relaxation in Solids* (Chelsea Dielectrics, London, 1983).
- [11] X. Chen, O. Sichelschmidt, W. Kleemann, O. Petravic, Ch. Binek, J. B. Sousa, S. Cardoso, and P. P. Freitas, Phys. Rev. Lett. **89**, 137203 (2002).
- [12] O. Petravic, A. Glatz, and W. Kleemann, Phys. Rev. B **70**, 214432 (2004).
- [13] S. Bedanta, O. Petravic, E. Kentzinger, W. Kleemann, U. Rücker, A. Paul, Th. Brückel, S. Cardoso, and P. P. Freitas, Phys. Rev. B **72**, 024419 (2005).
- [14] Th. Braun, W. Kleemann, J. Dec, and P. A. Thomas, Phys. Rev. Lett. **94**, 117601 (2005).
- [15] W. Kleemann, J. Dec, S. A. Prosandeev, T. Braun, and P. A. Thomas, Ferroelectrics **334**, 3 (2006).
- [16] A. I. Larkin and Yu. N. Ovchinnikov, J. Low Temp. Phys. **34**, 409 (1979).
- [17] A. Glatz, T. Nattermann, and V. Pokrovsky, Phys. Rev. Lett. **90**, 047201 (2003).
- [18] T. Nattermann, S. Stepanow, L.-H. Tang, and H. Leschhorn, J. Phys. II (France) **2**, 1483 (1992).
- [19] V. Mathet, T. Devolder, J. Ferré, S. Lemerle, L. Belliard, and G. Güntherodt, J. Magn. Magn. Mater. **260**, 295 (2003).
- [20] C. Chappert, H. Bernas, J. Ferré, V. Kottler, J. P. Jamet, Y. Chen, E. Cambri, T. Devolder, F. Rousseaux, V. Mathet, and H. Launois, Science **280**, 1919 (1998); J. Ferré, T. Devolder, H. Bernas, J. P. Jamet, V. Repain, M. Bauer, N. Vernier, and C. Chappert, J. Phys. D: Appl. Phys. **36**, 3103 (2003).
- [21] V. Repain, M. Bauer, J.-P. Jamet, J. Ferré, A. Mougin, C. Chappert, and H. Bernas, Europhys. Lett. **68**, 460 (2004).
- [22] N. L. Schryer and L. R. Walker, J. Appl. Phys. **45**, 5406 (1974).
- [23] P. J. Metaxas, J. P. Jamet, A. Mougin, M. Cormier, J. Ferré, V. Baltz, B. Rodmacq, B. Dieny, and R. L. Stamps, arXiv:cond.mat/0702654.